Nephrol Dial Transplant (2008) 23: 2198–2205
doi: 10.1093/ndt/gfn090
Advance Access publication 2 April 2008

Original Article

NDT
Nephrology Dialysis Transplantation

The molecular mechanisms of the attenuation of cisplatin-induced acute renal failure by *N*-acetylcysteine in rats

Jinghui Luo, Takayuki Tsuji, Hideo Yasuda, Yuan Sun, Yoshihide Fujigaki and Akira Hishida

First Department of Medicine, Hamamatsu University School of Medicine, Hamamatsu, Shizuoka, Japan

Abstract

Background. The clinical use of cisplatin (*cis*-diamminedichloro-platinum II, CDDP) is highly limited by its nephrotoxicity. Although *N*-acetylcysteine (NAC), a thiol-containing antioxidant, has been documented to be effective in attenuating renal injury induced by CDDP, the precise mechanisms involved in its renoprotection have not been completely clarified.

Methods. We investigated the effects of NAC on oxidative stress and oxidation-associated signals, such as p38 mitogen-activated protein kinase (MAPK), NF-κB and TNF-α, in CDDP-induced acute renal failure (ARF) rats, in comparison to the effects of melatonin (MT), one of the physiological TNF-α inhibitors, and pyrrolidine dithiocarbamate (PDTC), a NF-κB inhibitor.

Results. NAC blocked oxidative stress, p38 MAPK activation, caspase-3 cleavage, tissue apoptosis, renal dysfunction and morphological damage induced by CDDP. CDDP-triggered NF-κB translocation into the nucleus and TNF-α mRNA increase in the kidney were also inhibited in NAC-treated rats. MT downregulated the TNF-α mRNA level, and PDTC inhibited the increases in both NF-κB translocation and TNF-α mRNA. Neither MT nor PDTC were capable of interfering with oxidative stress, p38 MAPK phosphorylation, caspase-3 cleavage, tissue apoptosis and kidney injury induced by CDDP.

Conclusions. These data suggest that oxidative stress and p38 MAPK-mediated apoptotic cell death pathways are involved, at least in part, in the pathogenesis of CDDP-induced ARF, and negative regulation of p38 MAPK activation through inhibition of oxidative stress appears to play a central role in the beneficial effects of NAC.

Keywords: acute renal failure; cisplatin; *N*-acetylcysteine; p38 mitogen-activated protein kinase

Introduction

As a highly effective antitumour agent, cisplatin (*cis*-diamminedichloro-platinum II, CDDP) is used to treat a wide variety of malignant diseases. A serious adverse effect, nephrotoxicity, leading to acute renal failure (ARF), extremely limits the clinical use of the chemotherapeutic agent. Recent studies have also provided evidence supporting the involvement of p38 mitogen-activated protein kinase (MAPK) in ARF induced by both ischaemia/reperfusion [1] and renal toxicants including CDDP [2,3]. The MAPK pathways, including extracelluar signal-related kinase (ERK), c-Jun NH_2-terminal kinase (JNK) and p38 MAPK, are a series of parallel cascades of serine/threonin kinases that are activated by diverse extracellular, physical and chemical stresses and regulate cell proliferation, differentiation and survival. Among them, p38 MAPK is increasingly recognized as an important molecular component activated in response to a variety of stresses including oxidative stress [4], which is widely considered to play a central role in the development of ARF induced by CDDP. However, the mechanisms by which p38 MAPK activation results in renal damage in CDDP-induced ARF have not been well characterized.

Since the phosphorylated p38 MAPK can trigger apoptotic responses through direct activation of caspase-3 cascades [5], the direct activation of caspase-3 by phosphorylated p38 may cause apoptotic tubular cell death in CDDP-induced ARF. In contrast, some earlier studies have demonstrated that activation of p38 MAPK is involved in tumour necrosis factor-α (TNF-α) production and the nuclear factor-κB (NF-κB) activation [6–8], and at the same time, there are also reports indicating that CDDP treatment induces significant activation of NF-κB and remarkable increases in TNF-α production in kidneys, and the inhibition of NF-κB activation and TNF-α production is capable of attenuating CDDP-induced renal injury [9–11]. Therefore, it is possible that the activation of p38 MAPK may cause apoptosis through TNF-α production and/or NF-κB activation. On the other hand, there is accumulating evidence indicating that the disrupted oxidative status results in activation of various signalling molecules. NF-κB, in particular, is translocated into the nucleus

Correspondence and offprint requests to: Hideo Yasuda, First Department of Internal Medicine, Hamamatsu University School of Medicine, 1-20-1 Handayama, Hamamatsu, Shizuoka, 431-3192, Japan. E-mail: ysdh@hama-med.ac.jp, ysdh@mac.com

subjected to oxidative stress and then promotes the synthesis of inflammatory substances, including TNF-α [12], which has been regarded as an inducer of p38 MAPK activation [13–15]. Thus, it is also possible that oxidative stress-induced NF-κB activation or production of TNF-α is the cause of p38 MAPK phosphorylation. The exact roles of p38 MAPK, TNF-α and NF-κB and the interactions between these in the development of CDDP-induced ARF remain to be established.

N-Acetylcysteine (NAC), a thiol-containing antioxidant originally introduced as a mucolytic agent, is reported to have beneficial effects on renal injury induced by CDDP [11,16]. Data yielded *in vitro* have indicated that NAC can inhibit p38 MAPK activation, TNF-α biosynthesis [6,7,13–15] and NF-κB activation [17], and can block CDDP-induced apoptosis [18]. However, these inhibitory effects of NAC on p38 MAPK, TNF-α and/or NF-κB, which have been evaluated, are not clear *in vivo*. NAC is also a precursor of glutathione (GSH), which is reported to inhibit tubular injury by CDDP [19]. The *in vivo* mechanisms of NAC on CDDP-induced ARF have not been well evaluated.

To elucidate the possible roles of oxidative stress, p38 MAPK, TNF-α and NF-κB *in vivo* in CDDP-induced ARF and in the inhibition of CDDP toxicity by NAC, we investigated the effects of NAC, melatonin (5-methoxy-*N*-acetyl-tryptamine, MT), one of the physiological TNF-α production inhibitors [20,21], and pyrrolidine dithiocarbamate (PDTC), a NF-κB inhibitor, on the alternations of these intermediate signals and on the renal damage. In addition, another antioxidant, dimethylthiourea (DMTU), was used to exclude a specific substance effect of NAC on p38 MAPK pathways.

Subjects and methods

Experimental design

Male Sprague-Dawley rats weighing 220–250 g were purchased from SLC Co. (Shizuoka, Japan). Animals were housed under 12-h light/dark conditions at the temperature of 23 ± 2°C, and provided with standard rat chow and drinking water *ad libitum*.

ARF was induced by a bolus injection of CDDP (5 mg/kg i.v., Nippon Kayaku, Tokyo, Japan) dissolved in sterile 0.9% saline via the penile vein under light ether anaesthesia. Normal control rats received only isotonic saline.

Rats were divided into five different groups as follows: (1) saline-treated normal control rats and rats treated with CDDP (5 mg/kg, i.v.) plus intraperitoneal injection of (2) vehicle (5 ml/kg), (3) NAC (250 mg/kg), (4) MT (5 mg/kg) or (5) PDTC (80 mg/kg) once a day, with 6–9 rats in each group. The administration of the drugs started 2 days prior to a singe dose of CDDP. CDDP, NAC, MT or PDTC were dissolved in saline. As an additional experiment, five rats were injected with 500 mg/kg body weight of DMTU (Sigma-Aldrich, St. Louis, MO, USA) 1 h before the injection of CDDP, followed by the injection of 125 mg/kg body weight of DMTU twice a day [22]. At Day 5 after CDDP administration, blood samples were obtained from the abdominal aorta for measurement of the concentration of serum creatinine (Scr) using an enzymatic method (CreE test, Mizuho Medy, Saga, Japan), and kidneys were perfused with an ice-cold phosphate buffer solution (PBS) and removed for histological evaluation and immunohistochemistry; a portion of the outer stripe of the outer medulla (OSOM) was excised and frozen quickly in liquid nitrogen and stored at −80°C until required for analysis.

The experimental protocol was approved by the Ethics Review Committee for Animal Experimentation of Hamamatsu University School of Medicine.

Histological examination

Isolated perfused kidneys were fixed in 4% paraformaldehyde and embedded in paraffin. For histological evaluation of renal damage, 3-μm sections of renal tissue were counterstained with periodic acid Schiff (PAS) reagent. Because tubular damage was most evident in OSOM, a semiquantitative analysis was conducted on this area as described previously [23]. One hundred tubules were selected in 25 random fields (four tubules from the centre of each field) at ×400 magnification and scored for each rat. Each tubular profile was assigned to one of five categories according to the following criteria: 0, normal; 1, areas of tubular epithelial cell swelling, vacuolar degeneration, necrosis, and desquamation involving <20% of the tubular profile; 2, similar changes involving ≥20% but <40% of the tubular profile; 3, similar changes involving ≥40% but <60% of the tubular profile; 4, similar changes involving ≥60% but <80% of the tubular profile; 5, similar changes involving ≥80% of the tubular profile. To minimize observer bias, the morphometric examination was performed in a blinded fashion without knowledge of the treatment group from which the tissue originated. The mean score for each rat and the mean score for each group were then calculated.

The degree of apoptosis was assessed using a terminal uridine nick-end labelling (TUNEL) technique as described previously [24]. The tissue was deparaffinized and rehydrated, followed by incubation of 3-μm sections with 20 μg/ml proteinase K for 15 min and immersion in distilled water containing 3% hydrogen peroxide for 30 min at room temperature. Detection of DNA fragmentation was performed using ApoTag plus *in situ* Apoptosis Detection Kit (Oncor, Gaithersburg, MD, USA). A semiquantitative analysis was performed by counting TUNEL-positive cells per one field at ×400 magnification in OSOM. The mean number of stained cells in 20 randomly selected fields in each kidney was expressed as the number of TUNEL-positive cells.

For immunohistochemical examination of 8-OHdG expression, the paraffin samples were cut in 3-μm thickness, deparaffinized and rehydrated. After consuming endogenous peroxidase with 3% H_2O_2, slides were pre-incubated with 10% normal donkey serum to block non-specific reaction. The samples were incubated respectively with monoclonal mouse anti-8-OHdG (2 μm/ml) (Japan Institute for Control of Aging, Shizuoka, Japan) overnight at 4°C. After washing in PBS (pH 7.4), the samples were incubated with biotin-conjugated donkey anti-mouse IgG (Chemicon International, Temecula, CA, USA) for 30 min at room

temperature, washed in PBS, and then incubated with streptavidin-conjugated peroxidase for 30 min at room temperature. The reaction products were visualized using H_2O_2 containing 3,3′-diaminobenzidine in 0.05 M Tris buffer. The number of 8-OHdG-positive nuclei in OSOM was counted under a light microscope at ×400 magnification in 50 random fields in each experimental animal by an investigator who was blinded to the treatment, and its average value at each time point was calculated.

Measurement of renal GSH content

GSH content in OSOM was measured by GSH Detection Kit (BioVision, Mountain View, CA, USA) according to the manufacturer's instructions. In brief, the tissue sample (100 mg) was homogonized in 0.5 ml of glutathione reaction buffer containing 0.1 ml of 5% sulfosalicylic acid (SSA). To generate NADPH, 20 μl of NADPH Generating Mix and 140 μl glutathione reaction buffer were mixed and incubated at room temperature for 10 min. Then, 20 μl of either the GSH standard solution or the sample solution was added followed by incubation at room temperature for 5–10 min and further addition of 20 μl of substrate solution. The absorbance at 405 nm was read by a microplate reader. Protein content of each sample was determined by Bio-Rad Protein Assay kits (Bio-Rad Laboratories, Hercules, CA, USA).

Measurement of protein expression by western blot analysis

Isolation of whole fractions of proteins from OSOM was conducted by homogenizing kidneys in lysis buffer [1% (v/v) NP-40, 0.1% (w/v) SDS, 0.5% (w/v) sodium deoxycholate, 150 mM NaCl and 20 mM Tris–HCl, pH 8.0] in the presence of phenylmethylsulphonyl fluoride (PMSF) (1 μM), protease inhibitor cocktail (Sigma-Aldrich) and phosphatase inhibitor cocktail (Roche, Mannheim, Germany). The homogenate was centrifuged at 15 000 g for 20 min at 4°C and the supernatant was stored at −80°C until used for western blot analysis of cleaved caspase-3, phosphorylated-p38 (p-p38) MAPK, phosphorylated-ERK (p-ERK) and phosphorylated-JNK (p-JNK).

For western blot analysis of PARP-1, cleaved PARP-1 and NF-κB, nuclear extracts from OSOM of kidneys were prepared as described by Mehta *et al*. [25]. Tissues were homogonized in 500 μl of buffer A [Hepes (10 mM, pH 7.8), KCl (10 mM), $MgCl_2$ (2 mM), dithiothreiotol (0.5 mM), PMSF (1 mM), aprotinin (5 μg/ml), pepstatin A (5 μg/ml) and leupeptin (5 mg/ml)] containing NP-40 (0.1%), then stood on ice for 15 min, vortexed vigorously for 15 s and centrifuged at 14 000 rpm for 30 s. The pelleted nuclei were resuspended in 250 μl of buffer B [Hepes (20 mM, pH 7.9), glycerol (25% v/v), NaCl (0.4 M), $MgCl_2$ (1.5 mM), EDTA (0.2 mM), dithiothreiotol (0.5 m), PMSF (1 mM), aprotinin (5 μg/ml), pepstatin A (5 μg/ml) and leupeptin (5 μg/ml)]. After 30 min on ice, lysates were centrifuged at 14 000 rpm for 10 min again. Supernatants containing the nuclear proteins were collected and stored at −80°C until used.

Equivalent to 15 μg protein was separated on a Ready Gel System (Bio-Rad Laboratories, Hercules, CA, USA), and electroblotted onto Hybond ECL nitrocellulose membranes (Amersham Pharmacia Biotech UK, Bucks, UK). The membranes were blocked with 5% (w/v) skim milk powder in 0.1% (v/v) Tween-20 Tris-buffered saline for 1 h at room temperature. Blots were probed with prime antibodies of rabbit anti-cleaved caspase-3 (1:1000, Cell Signaling, Danvers, MA, USA), rabbit anti-PARP-1 and cleaved PARP-1 (1:1000, Cell Signaling), rabbit anti-p-p38 MAPK (1:200, Santa Cruz Biotechnology, Santa Cruz, CA, USA), mouse anti-pERK (1:500, Santa Cruz Biotechnology), mouse anti-p-JNK (1:1000, Cell Signaling) and rabbit anti-NF-κB (1:800, Abcam, Cambridge CB4 0FW, UK) at 4°C overnight. As an internal standard, blots were re-probed with mouse anti-β-actin mAb (1:50 000, Sigma-Aldrich) for 60 min at room temperature. Binding to primary antibodies was visualized using anti-rabbit or anti-mouse horseradish peroxidase at 1:10 000 dilution (Sigma-Aldrich) for 60 min at room temperature, followed by the ECL chemiluminescence detection system (Amersham Biosciences, Buckinghamshire, UK). Developed films were analysed semiquantitatively by JADE2 scanning densitometry and National Institutes of Health image-analysis software. The area under the scanning curve in each blot and the relative abundance of proteins were determined by dividing by each β-actin area.

Semiquantitative analysis of TNF-α mRNA by real-time RT-PCR

Total RNA was extracted from OSOM of the rat kidney using ISOGEN (Nippon Gene, Tokyo, Japan) according to the manufacturer's protocol. After treatment with DNase, we obtained poly-A+ enriched RNA by binding to oligo (dT) cellulose beads. The mRNA samples were quantified by spectrophotometry at 260 nm, and were reversibly transcribed into cDNA using a First Strand cDNA Synthesis Kit for reverse transcription-polymerase chain reaction (RT-PCR) (Roche, Mannheim, Germany). Real-time RT-PCR was performed in a Light Cycler (Roche, Grenzacherstrasse, Switzerland). All PCR experiments were performed using the QuantiTect SYBR Green PCR kit, purchased from QIAGEN (Tokyo, Japan). The amplification programmed consisted of 1 cycle at 95°C with a 7-min hold (hot start), followed by 40 cycles at 95°C with a 15-s hold, 58°C annealing temperature with a 5-s hold and 72°C with a 20-s hold. Amplification was followed by a melting curve analysis to verify the accuracy of the amplification. A Rat TNF-α Real Time PCR Primer Set (BioSource International, Carlsbad, CA, USA) was used, and positive and negative controls with mRNA were run to assess its specificity for reaction. For verification of the correct amplification, PCR products were analysed on an ethidium bromide-stained agarose gel.

Data analysis was performed using Light Cycler software, version 3.3.9, provided by Roche. After a melting curve analysis was carried out, standard curves for TNF-α and glyceraldehyde-3-phosphate-dehydrogenase (GAPDH) were generated by using PCR products of OSOM

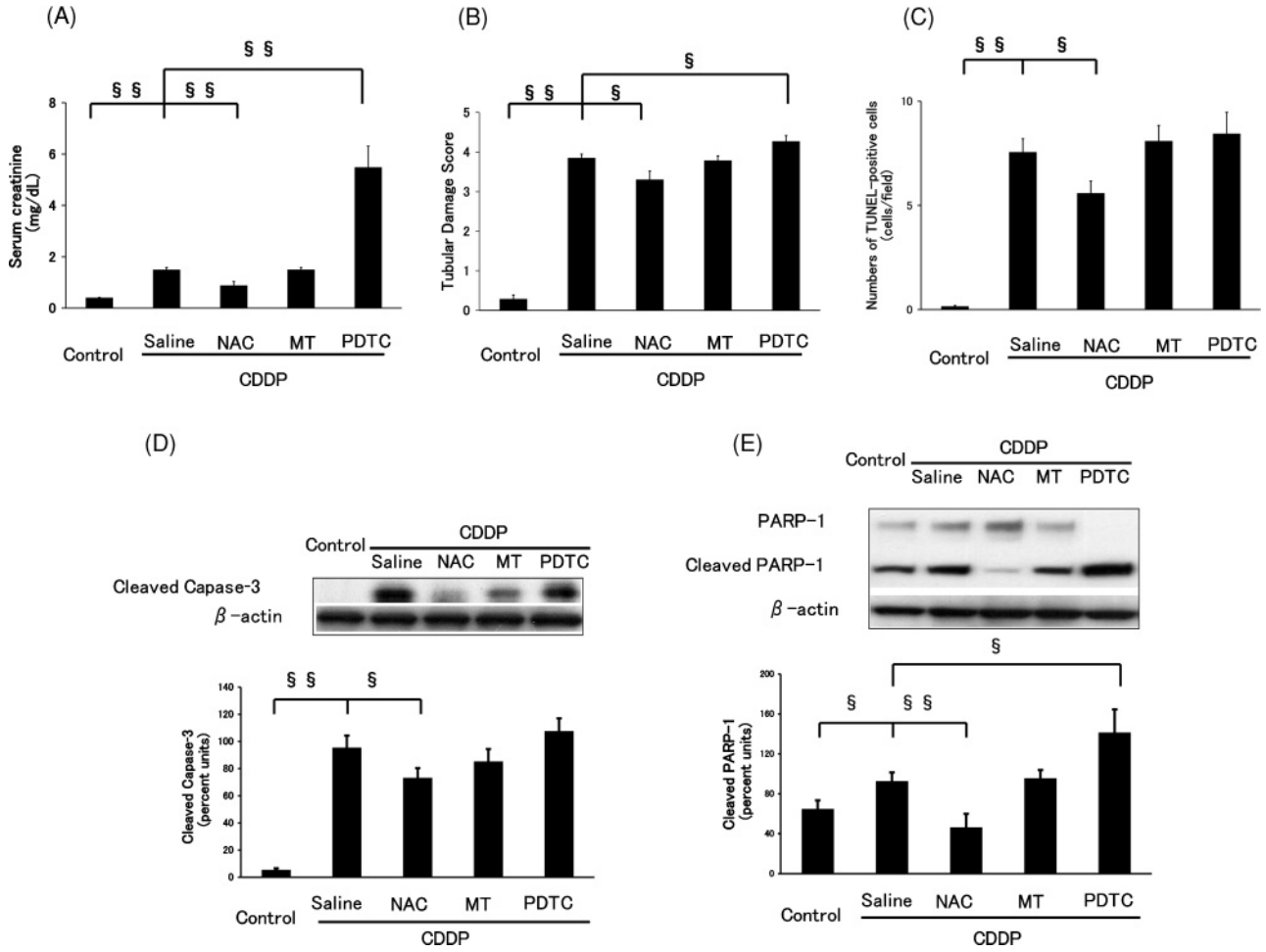

Fig. 1. Effects of NAC, MT and PDTC on serum creatinine (**A**), tubular damage score (**B**), the number of TUNEL-positive cells (**C**) and western blot analysis of cleaved caspase-3 (**D**) and cleaved PARP-1 expression (**E**) in OSOM on Day 5 after CDDP injection. Rats were treated with saline ($n = 6$), CDDP plus saline ($n = 6$), CDDP plus NAC ($n = 9$), CDDP plus MT ($n = 9$) or CDDP plus PDTC ($n = 9$) as shown in the Material and methods section. $^{\S\S}P < 0.01$, $^{\S}P < 0.05$.

mRNA as a template. The ratio of TNF-α mRNA to GAPDH mRNA was then calculated in each sample.

Statistical analyses

All data are presented as mean ± SEM. Significant differences among data were determined using one-way ANOVA with standard *post hoc* testing (Statview, version 5.0, Abacus Concepts, Berkeley, CA, USA). $P < 0.05$ denoted the presence of a statistically significant difference.

Results

The effects of NAC, MT and PDTC on CDDP-induced ARF

ARF model induced by a single CDDP-injection was characterized by markedly increased Scr at Day 5, with significant difference compared to the saline-treated group. Pretreatment with NAC 2 days before CDDP injection notably diminished the CDDP-induced increase in Scr. In contrast, PDTC treatment unfavourably augmented the increase in Scr. No remarkable effect on Scr was observed by MT injection (Figure 1A). Histological examination revealed extensive tubular epithelial detachment and casts of the lumen mainly in OSOM at Day 5 after CDDP administration. In accordance with the variation of Scr, the tubular damage caused by CDDP was significantly lessened by NAC, slightly but significantly augmented by PDTC, and unaffected by MT (Figure 1B). These findings indicate that NAC partially protects kidneys against CDDP-induced ARF, just as it has been documented. However, to our surprise, PDTC and MT, which were reported [26,27] to be effective in attenuating renal injury, were both found to be of no protection.

The number of TUNEL-positive cells was notably increased by CDDP at Day 5 after its injection. Treating the CDDP-induced ARF rats with NAC significantly decreased TUNEL-positive cells, but no significant change was observed when MT or PDTC was administered to CDDP-treated animals (Figure 1C).

The apoptotic process was also evaluated by detecting the cleavages of the downstream effecter caspase,

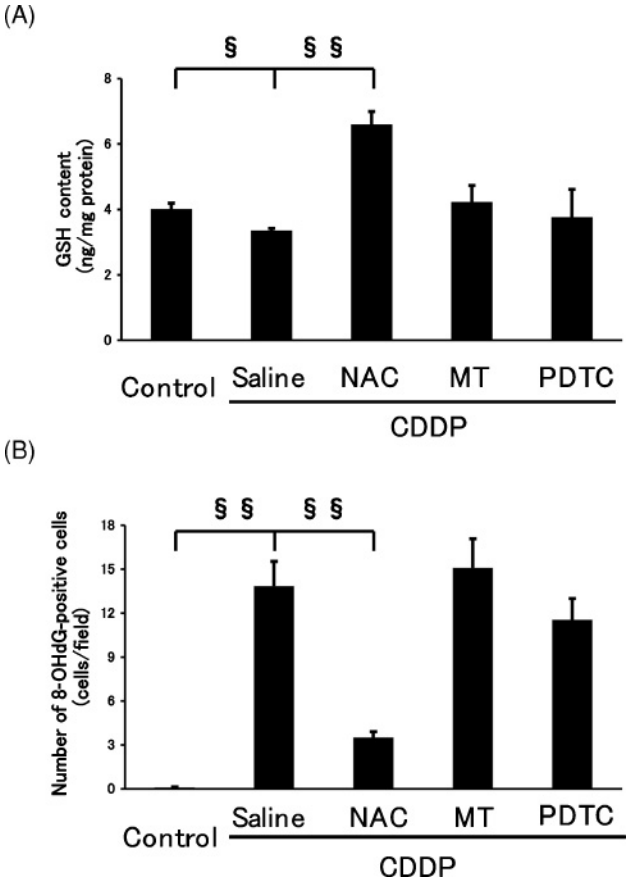

Fig. 2. GSH content (**A**) and the number of 8-OHdG-positive cells (**B**) in OSOM in CDDP-induced ARF in rats. Rats were treated with saline ($n = 6$), CDDP plus saline ($n = 6$), CDDP plus NAC ($n = 9$), CDDP plus MT ($n = 9$) or CDDP plus PDTC ($n = 9$) and killed 5 days after CDDP injection as described in the Material and methods section. $^{\S\S}P < 0.01$, $^{\S}P < 0.05$.

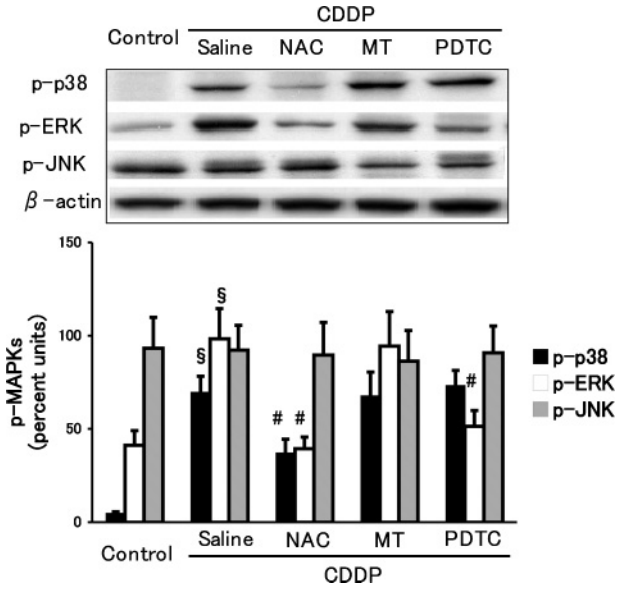

Fig. 3. Western blot analysis of phosphorylation of MAPKs in OSOM in CDDP-induced ARF in rats. Rats were treated with saline ($n = 6$), CDDP plus saline ($n = 6$), CDDP plus NAC ($n = 9$), CDDP plus MT ($n = 9$) or CDDP plus PDTC ($n = 9$) and killed 5 days after CDDP injection as described in the Material and methods section. $^{\S}P < 0.01$ versus saline-treated alone; $^{\#}P < 0.01$ versus (CDDP+saline)-treated.

caspase-3 and PARP-1, which is primarily cleaved by caspase-3 and described as an apoptosis marker. Significant increases in the cleavage of caspase-3 and PARP-1 were observed in CDDP-induced ARF (Figure 1D, E). NAC attenuated the CDDP-induced cleavage of caspase-3 and PARP-1, while MT did not affect the cleavage (Figure 1D, E). PDTC did not affect the cleavage of caspase-3 but the augmented cleavage of PARP-1 (Figure 1D, E).

The effects of NAC, MT and PDTC on oxidative stress evaluated by GSH and 8-OHdG

To evaluate the oxidative stress in CDDP-treated kidneys, we evaluated renal GSH level and 8-OHdG-positive cells. As the most abundant intracellular nonprotein thiol, GSH has been proved to be of great importance in the protection of cells against CDDP cytotoxicity [26]. CDDP injection significantly induced depletion of renal GSH, suggesting that oxidative stress was increased in the kidney by CDDP. Acting as a precursor of GSH synthesis, NAC not only drastically abolished but also significantly reversed the GSH decrease induced by CDDP (Figure 2A). In contrast, MT and PDTC did not induce a significant change in the GSH level when compared with CDDP alone (Figure 2A).

The 8-OHdG-positive cells evaluated in OSOM significantly increased in all CDDP-treated groups, when compared with normal kidneys (Figure 2B). Among them, NAC administrated ARF rats showed a significantly decreased number of renal 8-OHdG-positive cells compared with that of saline treated ARF animals, while MT or PDTC treatment did not affect the number of 8-OHdG-positive cells (Figure 2B).

These results confirm that disrupted oxidative status was induced in CDDP nephrotoxicity, and NAC, but not MT or PDTC, attenuated the CDDP-induced oxidative stress.

The effects of NAC, MT and PDTC on the phosphorylation of MAPKs

The activations of the redox-sensitive signals, p38 MAPK and JNK, and the reproliferation-related signal, ERK, in the kidney were detected. The phosphorylation of p38 MAPK and ERK, but not that of JNK, were substantially triggered by administration of CDDP. NAC significantly attenuated CDDP-induced phosphorylation of p38 MAPK and ERK (Figure 3). PDTC significantly suppressed the increase in p-ERK, but did not affect p-p38 MAPK (Figure 3). In addition, MT did not alter the CDDP-induced increases in p-MAPKs (Figure 3).

The effects of NAC, MT and PDTC on TNF-α mRNA abundance and NF-κB activation

CDDP evoked a considerable increase in TNF-α mRNA abundance in the kidney. Treating the rats with NAC,

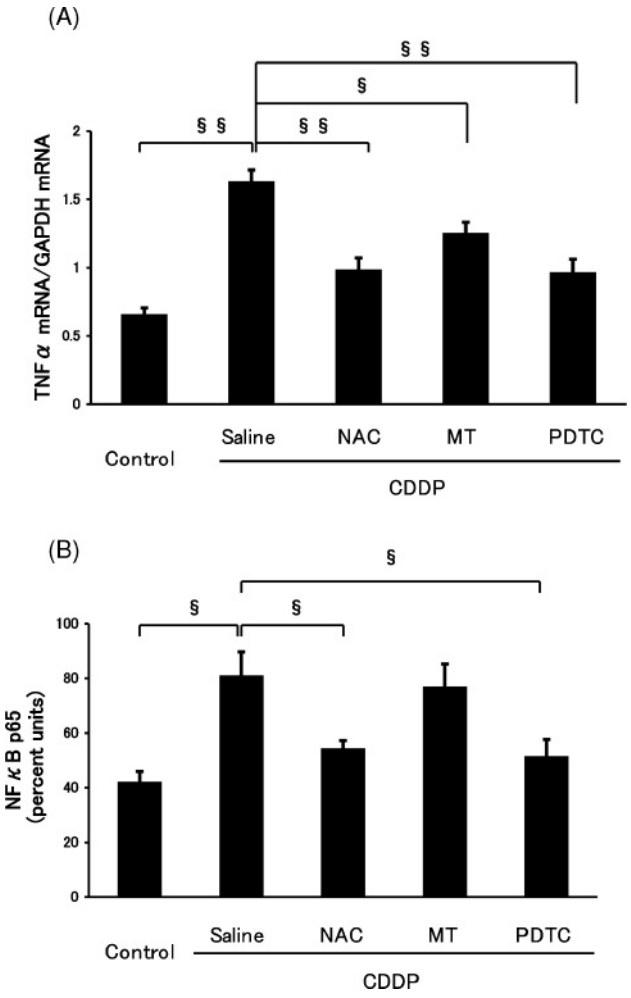

Fig. 4. Real-time RT-PCR analysis of TNF-α mRNA and western blot analysis of renal nuclear NF-κBp65 expression in OSOM in CDDP-induced ARF in rats. Rats were treated with saline ($n = 6$), CDDP plus saline ($n = 6$), CDDP plus NAC ($n = 9$), CDDP plus MT ($n = 9$) or CDDP plus PDTC ($n = 9$) as shown in Material and methods and killed 5 days after CDDP injection. $^{§§}P < 0.01$, $^{§}P < 0.05$.

MT and PDTC significantly lessened the increment (Figure 4A).

NF-κB activation was determined by measuring the nuclear NF-κBp65 protein level. The nuclear NF-κBp65 was increased by CDDP. NAC and PDTC significantly suppressed this increase ($P < 0.05$) (Figure 4B). In contrast, MT did not alter the CDDP-induced increase in nuclear NF-κBp65.

The effects of DMTU on CDDP-induced ARF and the phosphorylation of MAPKs

DMTU significantly decreased the Scr level (CDDP versus CDDP ± DMTU, 1.43 ± 0.13 versus 0.45 ± 0.02 mg/dl, $P < 0.05$) and the number of TUNEL-positive cells (CDDP versus CDDP ± DMTU, 4.49 ± 0.10 versus 1.22 ± 0.09/HPF, $P < 0.05$) at Day 5 after CDDP administration. DMTU also attenuated CDDP-induced phosphorylation of p38 MAPK and ERK (Figure 5).

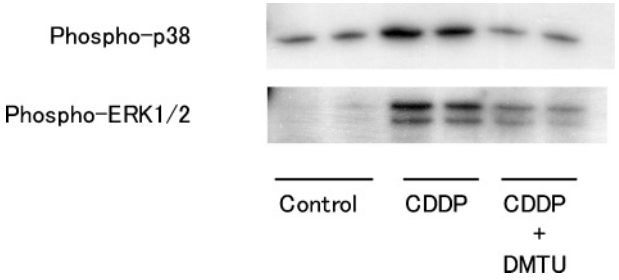

Fig. 5. Western blot analysis of DMTU on phosphorylation of p38 and ERK in OSOM in CDDP-induced ARF in rats. Rats were treated with saline ($n = 4$), CDDP plus saline ($n = 5$) and CDDP plus DMTU ($n = 5$) as shown in the Material and methods section and killed 5 days after CDDP injection. The blots shown in this figure were representative of two separate experiments.

Discussion

The present study revealed that (1) CDDP induced oxidative stress, p38 MAPK activation, caspase-3 cleavage, NF-κB translocation into nucleus, TNF-α mRNA increase, tissue apoptosis, renal dysfunction and morphological damage in rats; (2) NAC inhibited all these alterations in CDDP-treated rats; (3) MT downregulated the TNF-α mRNA level, and PDTC inhibited the increases in both NF-κB translocation and TNF-α mRNA level; (4) neither MT nor PDTC were capable of interfering with oxidative stress, p38 MAPK phosphorylation, caspase-3 cleavage, tissue apoptosis and kidney injury induced by CDDP; (5) CDDP enhanced phosphorylation of ERK, and NAC and PDTC significantly inhibited CDDP-induced activation of ERK; (6) no significant difference was found in p-JNK levels among CDDP, NAC, MT, PDTC and saline-injected model groups; (7) another anti-oxidant, DMTU, which is a hydroxyl radical scavenger, inhibited phosphorylation of p38 MAPK and ERK, tissue apoptosis and renal dysfunction. These results indicate that oxidative stress and p38 MAPK-mediated pathways are involved, at least in part, in the pathogenesis of CDDP-induced ARF, and negative regulation of p38 MAPK activation through inhibition of oxidative stress appears to play a central role in the beneficial effects of NAC. Since the dose of NAC used in this study is higher than clinically used dose recommendations, the applicability of the findings to the human setting needs further examination.

Accumulating evidence has proved that activation of p38 MAPK by CDDP and other chemotherapeutic agents, a downstream signal of reactive oxygen species (ROS), results in apoptotic cell death in cancer cells [28]. However, the role of p38 MAPK-mediated apoptosis of non-neoplastic cells in response to anticancer agents, including CDDP, remains to be established. The present study clearly demonstrated that CDDP induced oxidative stress, the phosphorylation of p38 MAPK and activation of apoptotic signals, and that NAC suppressed all of these alterations induced by CDDP. These results coincide with a study in porcine renal epithelial cells in which NAC reduced the CDDP-induced increase in phosphorylated p38 MAPK immunoreactivity [11]. In the current study, we observed a close relationship between oxidative stress and the activation of p38 MAPK, and between p38 MAPK and

caspase-3 activations. NAC reduced oxidative stress, phosphorylated p38 MAPK and cleaved caspase-3 in CDDP-treated kidneys. Another anti-oxidant, DMTU, also reduced phosphorylated p38 MAPK and tissue apoptosis, suggesting a possible exclusion of a specific substance effect of NAC on p38 MAPK pathways. Ramesh *et al*. [3] found that p38 MAPK was activated in mouse kidneys in response to CDDP, and DMTU abolished the increase in p38 MAPK phosphorylation in concert with the attenuation of renal damage in CDDP-induced ARF. They also demonstrated that p38 MAPK inhibitor, SKF-86002, attenuated CDDP nephrotoxicity in mice. In contrast, PDTC and MT, which did not affect the activation of p38 MAPK in CDDP-induced ARF, were incapable of inhibiting the cleavage of caspase-3. Similar cross-talk between p38 MAPK and caspase signalling cascade was also reported in CDDP-treated carcinoma cells [18]. All these results support the hypothesis that oxidative stress activates p38 MAPK, and in turn, mediates apoptosis in CDDP-induced ARF.

Recently, a crucial role for TNF-α in toxic and ischaemic ARF has been widely recognized [3,9,10,29]. Emerging data suggest that there is a link between p38 MAPK and TNF-α, but it is unclear whether TNF-α is an upstream signal of p38 MAPK or vice versa. Hashimoto *et al*. found that p38 MAPK, and consequent production of cytokines, was activated by TNF-α in vascular endothelial cells [13,14] and bronchial epithelial cells [15]. However, there were also some reports indicating that p38 MAPK blockage abrogated TNF-α production induced by CDDP in the kidney [3], or by lipopolysaccharide (LPS) in alveolar epithelial cells [6,7]. In the present study, despite their attenuation of the TNF-α mRNA level, MT and PDTC failed to alter phosphorylation of p38 MAPK, suggesting that p38 MAPK may be located upstream to TNF-α production. Our findings are in contrast to other reports in which critical effects of TNF-α were shown in CDDP-induced ARF [3,9,10,29]. Since ICAM-1 was upregulated in the kidneys of TNF-α-reduced mice by CDDP [30] and that inhibition of ICAM-1 by anti-CD54 attenuated CDDP-induced ARF [31], it is possible that other cytokines such as ICAM-1 may contribute to progression of CDDP-induced ARF in TNF-α-reduced rats treated with MT or PDTC. On the other hand, MT and PDTC might not suppress production of TNF-α protein sufficiently at the early phase of the present model though MT and PDTC decreased TNF-α mRNA.

As a regulator of the genes encoding inflammatory mediators, NF-κB is described to play a key role in a wide variety of diseases. The findings that NF-κB was activated by CDDP and NF-κB blockage led to protection against ARF have provided evidence to the opinion that activation of NF-κB plays a critical role in CDDP-induced ARF [10,32–34]. To date, available data imply a much more complicated relationship between NF-κB and p38 MAPK. Haddad *et al*. reported that the NF-κB inhibitor could partially hinder the p38 MAPK pathway [6], while Hayakawa *et al*. suggested that NF-κB was a downstream signal of p38 MAPK [35]. In contrast, the results yielded in neutrophils have suggested that NF-κB and p38 MAPK work independently [36]. To confirm the roles of NF-κB and evaluate the possible cross-talk between NF-κB and p38 MAPK in CDDP-induced ARF, we used PDTC, an NF-κB inhibitor. Despite its inhibitive effect, to almost the same extent as that of NAC, on renal NF-κB activation, PDTC did not alter activation of p38 MAPK, suggesting that p38 MAPK acts in an NF-κB independent manner. Furthermore, the findings that PDTC suppressed the activation of NF-κB but not the oxidative stress, p38 MAPK activation and renal damage in the current study suggest the crucial role of oxidative stress and p38 MAPK activation and the less important role of NF-κB activation in CDDP-induced ARF. Our current result is supported by the observation of Kim *et al*. [37] who found that the reduced malondialdehyde (MDA) level, rather than suppressed NF-κB activation, was responsible for prevention of CDDP nephrotoxicity. Likewise, it is possible that previously reported beneficial effects of NF-κB inhibition in CDDP-induced ARF [10,32–34] might be mediated by the inhibition of oxidation/p38 MAPK activation, but not NF-κB, because the oxidative status was found to be significantly improved in one of these studies [33], and p38 MAPK activation were not evaluated at all. In addition, accumulating data demonstrating that PDTC sensitizes both neoplastic and non-neoplastic cells to CDDP-induced apoptosis [38,39] are in line with our result that PDTC augmented, rather than ameliorated, CDDP-induced apoptosis and ARF.

Based on previous findings of the participation of MAPKs in cell injury, it is suggested that p38 and JNK promote apoptotic cell death; in contrast, ERK is more likely responsible for cell proliferation [4,27]. It is also reported that JNK is associated with TNF-α-induced apoptosis [40]. In our experiment, in response to CDDP, phosphorylation of p38 and ERK, but not JNK, was markedly augmented in the kidney, and the modification of TNF-α mRNA expression by NAC, MT or PDTC did not affect the JNK phosphorylation. These results suggest that TNF-α-mediated modification of JNK phosphorylation may not be an essential event in CDDP-induced apoptotic cell death. Jo *et al.* [41] reported that the MAPK/ERK kinase inhibitor, U0126, attenuated CDDP-induced renal injury in mice. In this study, NAC and PDTC significantly inhibited CDDP-induced activation of ERK. However, only NAC decreased apoptosis and attenuated renal injury, suggesting that NAC but PDTC could inhibit ERK pathway sufficiently or that less contribution of ERK in CDDP-induced ARF in rats. In the current study, however, phosphorylation of MAPKs was only measured in kidneys 5 days after CDDP treatment. The role of MAPKs in the early stage of ARF, therefore, remains to be verified.

In summary, our current data suggest a critical role for oxidative stress and consequent activation of p38 PAMK in the induction of apoptosis and the pathogenesis of CDDP-induced ARF, and that the improvement of oxidative status and the inactivation of p38 MAPK are closely related to the renoprotective action of NAC. Furthermore, enhanced NF-κB activation and increased TNF-α mRNA seem to be of less significance in renal damage provoked by CDDP.

Acknowledgements. We thank Nippon Kayaku Co. Ltd (Tokyo, Japan) for kindly providing the CDDP for this study. This research was partially supported by Japan–China Medical Sasagawa Fellowship.

Conflict of interest statement. None declared.

References

1. Li R, Ding T, Liu X *et al*. Influence of SB203580 on cell apoptosis and P38 MAPK in renal ischemia/reperfusion injury. *J Huazhong Univ Sci Technolog Med Sci* 2006; 26: 50–52
2. Volpini RA, Balbi AP, Costa RS *et al*. Increased expression of p38 mitogen-activated protein kinase is related to the acute renal lesions induced by gentamicin. *Braz J Med Biol Res* 2006; 39: 817–823
3. Ramesh G, Reeves WB. p38 MAP kinase inhibition ameliorates cisplatin nephrotoxicity in mice. *Am J Physiol Renal Physiol* 2005; 289: F166–F174
4. Chang L, Karin M. Mammalian MAP kinase signalling cascades. *Nature* 2001; 410: 37–40
5. Jiang DJ, Jia SJ, Dai Z *et al*. Asymmetric dimethylarginine induces apoptosis via p38 MAPK/caspase-3-dependent signaling pathway in endothelial cells. *J Mol Cell Cardiol* 2006; 40: 529–539
6. Haddad JJ. The involvement of L-gamma-glutamyl-L-cysteinyl-glycine (glutathione/GSH) in the mechanism of redox signaling mediating MAPK(p38)-dependent regulation of pro-inflammatory cytokine production. *Biochem Pharmacol* 2002; 63: 305–320
7. Haddad JJ, Land SC. Redox/ROS regulation of lipopolysaccharide-induced mitogen-activated protein kinase (MAPK) activation and MAPK-mediated TNF-alpha biosynthesis. *Br J Pharmacol* 2002; 135: 520–536
8. Sakai N, Wada T, Furuichi K *et al*. p38 MAPK phosphorylation and NF-kappa B activation in human crescentic glomerulonephritis. *Nephrol Dial Transplant* 2002; 17: 998–1004
9. Ramesh G, Reeves WB. TNF-alpha mediates chemokine and cytokine expression and renal injury in cisplatin nephrotoxicity. *J Clin Invest* 2002; 110: 743–745
10. Ramesh, G, Reeves WB. Salicylate reduces cisplatin nephrotoxicity by inhibition of tumor necrosis factor-alpha. *Kidney Int* 2004; 65: 490–499
11. Mishima K, Baba A, Matsuo M *et al*. Protective effect of cyclic AMP against cisplatin-induced nephrotoxicity. *Free Radic Biol Med* 2006; 40: 1564–1577
12. Gloire G, Legrand-Poels S, Piette J. NF-kappaB activation by reactive oxygen species: fifteen years later. *Biochem Pharmacol* 2006; 72: 1493–1505
13. Hashimoto S, Gon Y, Matsumoto K *et al*. *N*-Acetylcysteine attenuates TNF-alpha-induced p38 MAP kinase activation and p38 MAP kinase-mediated IL-8 production by human pulmonary vascular endothelial cells. *Br J Pharmacol* 2001; 132: 270–276
14. Hashimoto S, Gon Y, Matsumoto K *et al*. Regulation by intracellular glutathione of TNF-alpha-induced p38 MAP kinase activation and RANTES production by human pulmonary vascular endothelial cells. *Allergy* 2000; 55: 463–469
15. Hashimoto S, Gon Y, Matsumoto K *et al*. Intracellular glutathione regulates tumor necrosis factor-alpha-induced p38 MAP kinase activation and RANTES production by human bronchial epithelial cells. *Clin Exp Allergy* 2001; 31: 144–151
16. Dickey DT, Wu YJ, Muldoon LL *et al*. Protection against cisplatin-induced toxicities by *N*-acetylcysteine and sodium thiosulfate as assessed at the molecular, cellular, and *in vivo* levels. *J Pharmacol Exp Ther* 2005; 314: 1052–1058
17. Li YQ, Zhang ZX, Xu YJ *et al*. *N*-Acetyl-L-cysteine and pyrrolidine dithiocarbamate inhibited nuclear factor-kappaB activation in alveolar macrophages by different mechanisms. *Acta Pharmacol Sin* 2006; 27: 339–346
18. Wu YJ, Muldoon LL, Neuwelt EA. The chemoprotective agent *N*-acetylcysteine blocks cisplatin-induced apoptosis through caspase signaling pathway. *J Pharmacol Exp Ther* 2005; 312: 424–131
19. Satoh M, Shimada A, Zhang B *et al*. Renal toxicity caused by cisplatinum in glutathione-depleted metallothionein-null mice. *Biochem Pharmacol* 2000; 60: 1729–1734
20. Lissoni P. The pineal gland as a central regulator of cytokine network. *Neuro Endocrinol Lett* 1999; 20: 343–349
21. Mazzon E, Esposito E, Crisafulli C *et al*. Melatonin modulates signal transduction pathways and apoptosis in experimental colitis. *J Pineal Res* 2006; 41: 363–373
22. Matsushima H, Yonemura K, Ohishi K *et al*. The role of oxygen free radicals in cisplatin-induced acute renal failure in rats. *J Lab Clin Med* 1998; 131: 518–526
23. Miyaji T, Kato A, Yasuda H *et al*. Role of the increase in p21 in cisplatin-induced acute renal failure in rats. *J Am Soc Nephrol* 2001; 12: 900–908
24. Zhou H, Miyaji T, Kato A *et al*. Attenuation of cisplatin-induced acute renal failure is associated with less apoptotic cell death. *J Lab Clin Med* 1999; 134: 649–658
25. Mehta A, Sekhon CP, Giri S *et al*. Attenuation of ischemia/reperfusion induced MAP kinases by *N*-acetyl cysteine, sodium nitroprusside and phosphoramidon. *Mol Cell Biochem* 2002; 240: 19–29
26. de Jesus Soares T, Costa RS, Balbi AP *et al*. Inhibition of nuclear factor-kappa B activation reduces glycerol-induced renal injury. *J Nephrol* 2006; 19: 439–448
27. Parlakpinar H, Sahna E, Ozer MK *et al*. Physiological and pharmacological concentrations of melatonin protect against cisplatin-induced acute renal injury. *J Pineal Res* 2002; 33: 161–166
28. Olson JM, Hallahan AR. p38 MAP kinase: a convergence point in cancer therapy. *Trends Mol Med* 2004; 10: 125–129
29. Daemen MA, vande Ven MW, Heineman E *et al*. Involvement of endogenous interleukin-10 and tumor necrosis factor-alpha in renal ischemia-reperfusion injury. *Transplantation* 1999; 67: 792–800
30. Ramesh G, Reeves WB. TNF-alpha mediates chemokine and cytokine expression and renal injury in cisplatin nephrotoxicity. *J Clin Invest* 2002; 110: 835–842
31. Kelly KJ, Meehan SM, Colvin RB *et al*. Protection from toxicant-mediated renal injury in the rat with anti-CD54 antibody. *Kidney Int* 1999; 56: 922–931
32. Lee S, Kim W, Moon SO *et al*. Rosiglitazone ameliorates cisplatin-induced renal injury in mice. *Nephrol Dial Transplant* 2006; 21: 2096–2105
33. Lee S, Moon SO, Kim W *et al*. Protective role of L-2-oxothiazolidine-4-carboxylic acid in cisplatin-induced renal injury. *Nephrol Dial Transplant* 2006; 21: 2085–2095
34. Li S, Gokden N, Okusa MD *et al*. Anti-inflammatory effect of fibrate protects from cisplatin-induced ARF. *Am J Physiol Renal Physiol* 2005; 289: F469–F480
35. Hayakawa K, Meng Y, Hiramatsu N *et al*. Spontaneous activation of the NF-kappaB signaling pathway in isolated normal glomeruli. *Am J Physiol Renal Physiol* 2006; 291: F1169–F1176
36. Cloutier A, Ear T, Blais-Charron E *et al*. Differential involvement of NF-kappaB and MAP kinase pathways in the generation of inflammatory cytokines by human neutrophils. *J Leukoc Biol* 2007; 81: 567–577
37. Kim SH, Hong KO, Hwang JK *et al*. Xanthorrhizol has a potential to attenuate the high dose cisplatin-induced nephrotoxicity in mice. *Food Chem Toxicol* 2005; 43: 117–122
38. Venkatraman M, Anto RJ, Nair A *et al*. Biological and chemical inhibitors of NF-kappaB sensitize SiHa cells to cisplatin-induced apoptosis. *Mol Carcinog* 2005; 44: 51–59
39. Cardoso SM, Oliveira CR. Inhibition of NF-κB renders cells more vulnerable to apoptosis induced by amyloid beta peptides. *Free Radic Res* 2003; 37: 967–973
40. Ding WX, Yin XM. Dissection of the multiple mechanisms of TNF-alpha-induced apoptosis in liver injury. *J Cell Mol Med* 2004; 8: 445–454
41. Jo SK, Cho WY, Sung SA *et al*. MEK inhibitor, U0126, attenuates cisplatin-induced renal injury by decreasing inflammation and apoptosis. *Kidney Int* 2005; 67: 458–466

Received for publication: 21.6.07
Accepted in revised form: 30.1.08